# UNDERWATER PHOTOGRAMMETRIC VERIFICATION OF NUCLEAR FUEL ASSEMBLIES VIA NATURAL FEATURE MEASUREMENT

Kenneth Edmundson
Geodetic Systems, Inc.
1511 Riverview Dr.
Melbourne, Florida 32901-4625
USA
kle@geodetic.com

Giuseppe Ganci
Gancell Pty. Ltd.
27 Browning Street
Moonee Ponds, Victoria 3039,
Australia
gganci@geodetic.com

Park, Chan-Hong
VisionTech, Inc.
61-3 Lifeofficetel B/D
826 Yoidodong,
YoungdeungpoGu, Seoul, Korea
shinsng@yahoo.co.kr

## ABSTRACT

This paper describes the underwater photogrammetric measurement of fuel assemblies in a nuclear reactor vessel. Geodetic Systems, Inc. (GSI), in conjunction with VisionTech, Inc. and Gancell Pty. Ltd., was requested to perform this task at the Yonggwangg Nuclear Power Plant in South Korea by Korea Hydro & Nuclear Power Co., Ltd. (KHNP). The environment of the reactor core, submerged and radioactive, poses a number of difficulties to the photogrammetrist. For protection in the underwater setting, a watertight canister with a quartz window was designed to house the camera. The multiple mediums of water, quartz, and air through which light must travel in its path to the camera add complexity to the traditional collinearity model of photogrammetric reconstruction. Artificial targets of either white or retro-reflective material, commonly used to signalize points of interest in industrial photogrammetry, cannot be placed on the fuel assemblies. Therefore, the detection and measurement of the natural features of the assembly itself becomes necessary. In turn, scene illumination, image exposure, and camera movement are important considerations. In the following, requirements of the measurement are outlined, along with brief descriptions of the design of the reactor core, fuel assemblies, and the underwater canister created for this application. The detection and measurement of the fuel assemblies are explained, followed by details and results of an actual measurement. In conclusion, potential extensions of the technique to other applications are described.

## 1  INTRODUCTION

In early 2004, Korea Hydro & Nuclear Power Co., Ltd. (KHNP) approached VisionTech, Inc. of Seoul in the Republic of Korea for assistance with the measurement of fuel assemblies in a nuclear reactor vessel. VisionTech, a partner of Geodetic Systems, Inc. (GSI), in turn requested that GSI, with the assistance of Gancell Pty. Ltd. of Australia, develop the necessary software, hardware, and procedures to perform this measurement. In March of 2006, the system developed for this task was successfully demonstrated at the Yonggwangg Nuclear Power Plant on the southwest coast of the Republic of Korea.

The Yonggwangg facility is a Korean Standard Nuclear Power Plant (KSNP). Refueling outages typically take place at intervals of 12-24 months. Refueling involves removing a number of spent fuel assemblies and loading an equal number of fresh assemblies. It is critical that the fuel assemblies be in their proper location when the top of the reactor is lowered into place.  Any that fall outside of the allowable tolerance may result in interference and potential damage to the assembly, the top of the reactor vessel, or both. This in turn could lead to an unplanned, and very costly extended outage. Moreover, after refueling, the nuclear and thermal characteristics, and the safety and operating

parameters of the core will be different from those prior to refueling (Zee, n.d.). For these reasons, it is necessary to establish the relative positions of the fuel assemblies. While rudimentary methods have been used to accomplish this, to date no accurate, efficient, and automated approach has been forthcoming. The need for such an approach has been desired for several years.

State-of-the-art photogrammetric systems, supported by digital camera technology and computer vision techniques, offer an attractive solution to the problem. The measurement of the fuel assemblies is, however, a difficult task for several reasons. The environment is hazardous. The assemblies lie 12 meters underwater and are radioactive. This presents both physical and mathematical challenges. To work underwater, the camera must be housed in a watertight canister. To work online, power and communications must be provided from the surface to the camera, through the canister. Imaging underwater complicates the traditional collinearity model of photogrammetric reconstruction as light must travel through water, air, and the canister window.

Typically in industrial photogrammetry, artificial targets of either white or retro-reflective material are used to signalize points of interest on the object to be measured. Here, targets cannot be placed on the fuel assemblies. Therefore, it is necessary to detect and measure the natural features of the assembly itself. It follows that scene illumination, image exposure, and camera movement are important considerations.

In the following, the designs of the reactor core and fuel assemblies are described and the measurement requirements are outlined. The design of the underwater camera canister created for this application is detailed. The detection and measurement of the fuel assemblies are explained, followed by a description and results of an actual measurement.

## 2 THE KSNP REACTOR CORE AND FUEL ASSEMBLY DESIGN

The following description of the KSNP reactor core design follows closely Zee (n.d.). The KSNP utilizes a pressurized water reactor. The reactor core consists of 177 fuel assemblies positioned to approximate a right circular cylinder with a diameter of three meters (Figure 1).

An individual fuel assembly, 4.5 meters long, has 236 fuel rod positions in a 16x16 array, five guide tubes welded to spacer grids, and is enclosed by end fittings at the top and bottom (Figure 2). It is the top surfaces (or hold-down plates) of the upper end fittings (UEFs) that are to be measured. They are assumed to lie in a plane approximately 12 meters below the surface of the water in the reactor vessel.

The UEF plate (Figure 1 inset and Figure 2 upper right) is of single-piece construction and consists of five connected rings, through which pass the guide tubes. The central guide ring is attached to four surrounding rings positioned at 45°, 135°, 225°, and 315°. The central and surrounding rings have outer diameters of 50 mm and 62 mm respectively. The center-to-center distance between adjacent outer rings is 102.87 mm.

## 3 FUEL ASSEMBLY MEASUREMENT REQUIREMENTS

It is necessary to provide measurements for the center points of the five rings of each UEF plate in the XY plane only. Thus, with 177 fuel assemblies, 885 points must be measured. The required point-to-point accuracy is stated at 0.76 mm (one-sigma) in X and Y. Illumination is to be from temporary underwater lights, positioned around the upper interior of the reactor vessel.

In August 2004 a mock test measurement was completed in which six fuel assembly UEF plates were measured in air. Albeit rudimentary, the results indicated that the measurement requirements outlined by KHNP could be met. In February 2005, GSI,
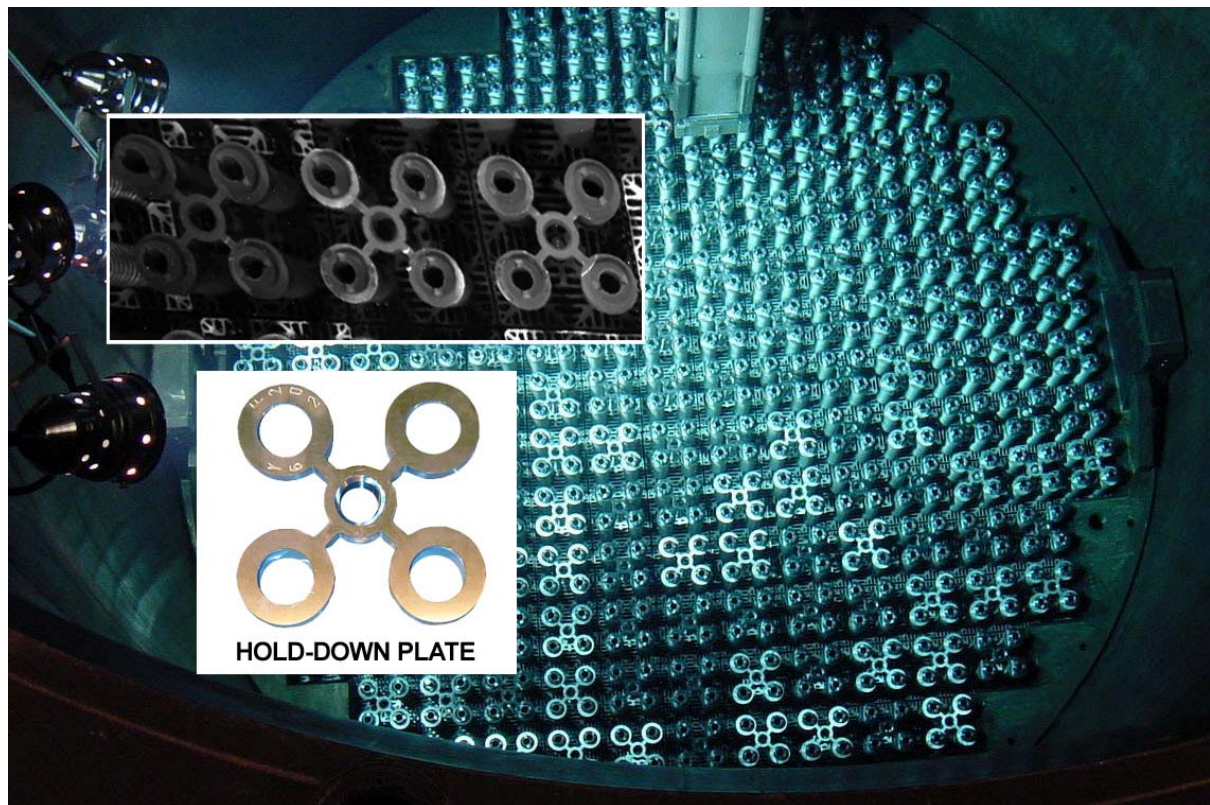


**Figure 1: Fuel assemblies in KSNP reactor core. Upper inset details the fuel assembly upper end fitting. Lower inset shows the upper end fitting (UEF) hold-down plate.**
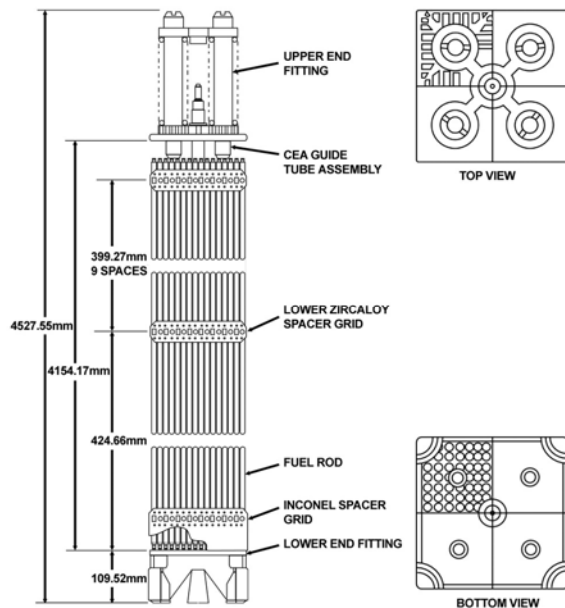
**Figure 2: KSNP fuel assembly. Plan view of upper end fitting is shown at upper right. After Zee (n.d.).**

Gancell Pty. Ltd., and VisionTech, Inc. commenced work on a solution to the problem.

## 4 HARDWARE

### 4.1 Camera

As image acquisition would be performed underwater, a photogrammetric camera that could be controlled remotely was required.

GSI's INCA3 camera receives power and communications via a combined power / ethernet cable. Functions such as strobe power, shutter speed and camera triggering are controlled through the V-STARS software installed on the host computer. Upon acquisition, the image is compressed and then transferred by ethernet to the host computer where it can be examined, measured, or re-acquired if necessary. The camera can also be powered up or down remotely.

The INCA series of cameras has an extensive history of use within canister environments. The I-CAN (INCA Canister) was developed in 1997 for use in thermal vacuum chamber measurements. This experience was utilized in the development of an underwater canister for the INCA3.

### 4.2 Underwater Canister

One of the first requirements of the project was the development of an underwater canister suitable to house the INCA3 camera. A number of off-the-shelf options were considered, but due to various functionality restrictions it was necessary to build a custom housing.

The primary concern with building a custom housing was the time needed to complete design and construction. The project test phases would all coincide with outages planned well in advance. As such, there was no flexibility in rescheduling the test to suit delivery. With the next outage scheduled for June 2005, the challenge was to find an engineering firm with the necessary expertise to design, manufacture, and test the canister in the limited time available.

Although there are a number of engineering firms specializing in underwater engineering applications around the world, finding a firm to design and manufacture the canister in time proved difficult. Fortunately, Underwater Video Systems of Perth, Australia was able to provide a suitable solution in the required time frame.

The final canister design was kept as simple as possible to minimize manufacturing cost, as well as to allow the demanding delivery schedule to be met. The canister was made up of three principal components, the main body and two end plates which seal the housing (Figure 3).

The main body was constructed of a solid piece of 16mm aluminum rolled and welded to a prescribed diameter based on the size of the INCA3 camera. The front plate encloses the camera window. The window is made from a piece of non-browning fused silica selected for its radiation resistance. This type of glass is typically used in radioactive environments to avoid discoloration when exposed to radiation. The rear plate includes a mounting bracket with a Manfrotto quick release mechanism to hold the camera in place. Both end plates feature double rubber o-rings for redundancy to ensure a water tight canister. As an added precaution, a leak detector alarm was installed in the unlikely event that the housing seal is



**Figure 3: INCA3 and underwater canister.**

breached.

Power and communications are provided to the camera through the canister via a standard 30m cable. This cable is specially wrapped in a Polyurethane jacket to make it suitable for use in an underwater nuclear environment.

### 4.3 Camera Motion Control

A suitable canister design having been selected, the problem of moving the camera underwater was addressed. The optimal network design, given the restrictive environment, consists of a minimum of nine camera stations arranged in a regular grid three meters above the plane of the UEF plates. Two images are acquired at each camera station with a 90 degree roll between them about the camera axis. This facilitates camera self-calibration. To position the camera at the correct height above the UEF plates, the canister is attached at the end of a series of interlocking poles and then lowered into the reactor vessel (Figure 4). The upper end of the assembled pole is mounted to the side safety rail of the overhead refueling machine bridge (Figure 5). The overhead bridge then shuttles the camera over the UEFs. The pole is initially attached to one end of the bridge and sweeps across the reactor vessel, stopping at three stations to acquire imagery. The pole is then moved to the center of the bridge and makes a second pass. Finally, the pole is attached to the opposite end of the bridge and makes a third and final pass.

In the initial canister design, an internal roll mechanism was considered to achieve the 90 degree roll about the camera axis. This was discounted due to the difficulty in engineering such a device within the limited time frame available and to the weight it would add to an already heavy design. A specialized underwater pan/tilt device with the necessary weight rating was selected which would allow the camera to
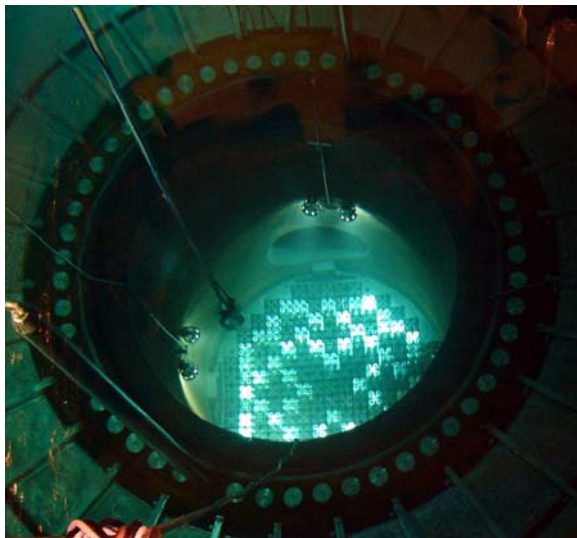


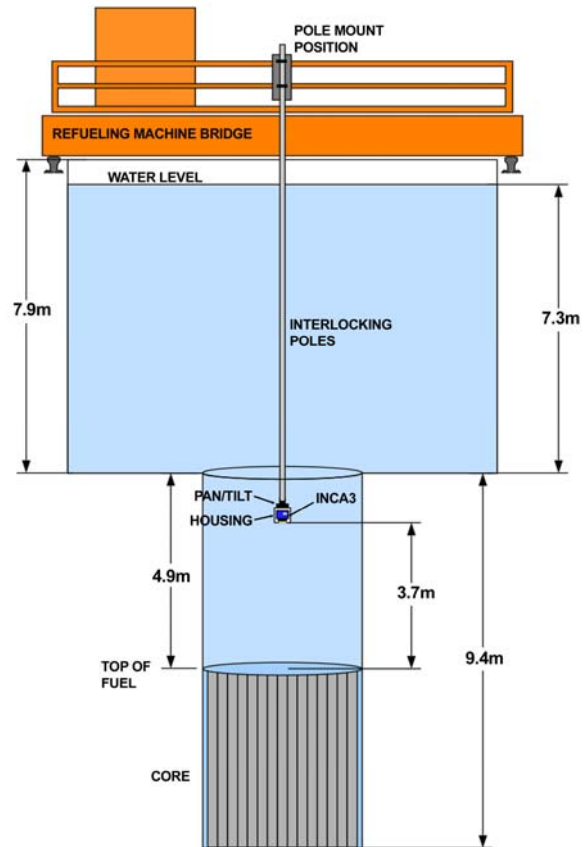**Figure 4: Camera lowered into reactor vessel.**



**Figure 5: Reactor core diagram with camera, interlocking poles, and refueling machine bridge.**

be rotated about its axis as well as tilted up to nearly 90 degrees from the vertical (Figure 6).

## 5  INITIAL TESTING

With the underwater canister completed in time for the next outage, a test date was set. The primary objective was to collect sufficient test imagery to facilitate software development for the measurement of the rings on each UEF.

The camera was sealed in the canister and a series of functionality tests were successfully completed. The camera and canister were brought into the chamber, attached to the assembled pole, and lowered underwater adjacent to the main pool. Test images were collected to establish the exposure and shutter speed needed to image the natural features of the UEF plates. Initial imagery was not as sharp as expected due to an air pocket trapped over the glass window when the camera was lowered into the pool. The canister was tilted to its maximum angle to allow the air to escape. Subsequent images were clear and in sharp focus.

To obtain a clear, high contrast image of the UEF plate, a significantly longer shutter speed is required than when measuring retro-reflective targets. This in turn makes camera stability during exposure a primary concern. In photogrammetric surveys
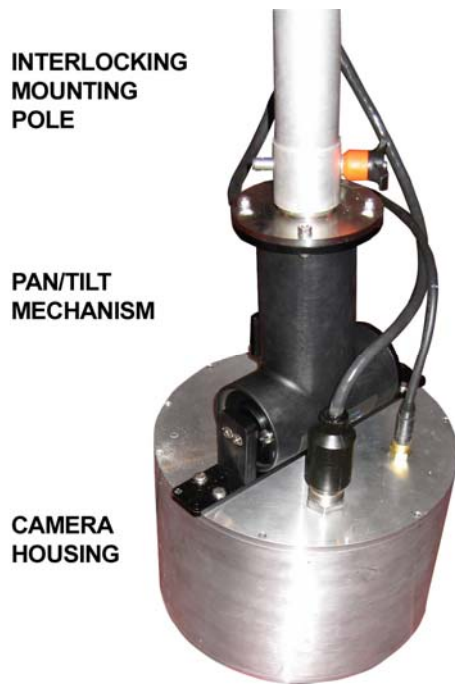
**Figure 6: Camera canister pole mount with pan/tilt mechanism.**

utilizing retro-reflective targeting, stability is typically not an issue. Since the targets are imaged stroboscopically, blurring in the image background has no effect on the photogrammetric accuracy of the targeted points. For imaging natural features, however, a crisp image with good contrast is imperative.

At shutter speeds greater than 50 milliseconds even slight movement will cause image blur. In this test, shutter speeds from 500 to 2000 milliseconds were considered. With the camera hanging 9 meters below, any bridge movement resulted in significant motion at the canister. After each movement of the bridge it was necessary to wait until the canister ceased moving. Fortunately, the water acts as a dampening force, stopping the motion in about 30 seconds.

Image contrast is another notable issue. After loading, the reactor core contains fuel assemblies of varying age. This is visibly apparent when looking at the UEF plates. As shown in Figure 7, the new plates are bright and shiny whilst the older ones are dull with a dark patina. At long exposures the new plates are very reflective and cause localized image saturation. At shorter exposures the new plates are not saturated, but the older plates appear dim and hard to distinguish from the background. The compromise for shutter speed seemed to be 1000 milliseconds. At this shutter speed the new plates were bright but not saturated. The old plates were dim, but distinguishable. For future measurements it

may be necessary to take two sets of images at different exposures and then combine the data sets.

During the course of the image collection it was noted that the images were becoming progressively darker. Eventually the level of contrast reached a point where the features were no longer discernible. It was feared that the camera electronics had been damaged by radioactivity or by water that may have penetrated the canister. Approximately 30 images had been collected and it was decided to stop the test in hopes of avoiding irreparable damage to the camera.

The canister was removed from the water and opened. Upon touching the camera it was immediately clear that the camera's operating temperature range had been exceeded. The surface temperature of the camera shell was estimated at 55 degrees Celsius. The interior would likely be even hotter.

It was surmised that the contrast problem was likely related to heat build-up in the canister and not radiation or water damage. The water temperature in the pool is approximately 30 degrees Celsius. Combined with the heat generated by the camera, the inside temperature rose continuously until the operating temperature of the CCD sensor had been exceeded. After being allowed to cool, the camera returned to normal operation. It should be noted that the camera had been powered continuously for approximately three hours. In future tests the camera will be switched off when not in use, significantly reducing heat build-up and thus eliminating the contrast problems.

# 6 MEASUREMENT BY DETECTION OF SIGNALIZED POINTS

The standard measurement procedure when using targets in close-range, industrial photogrammetry has been well-documented (Fraser, 1997). It is described briefly here for comparison with the measurement of
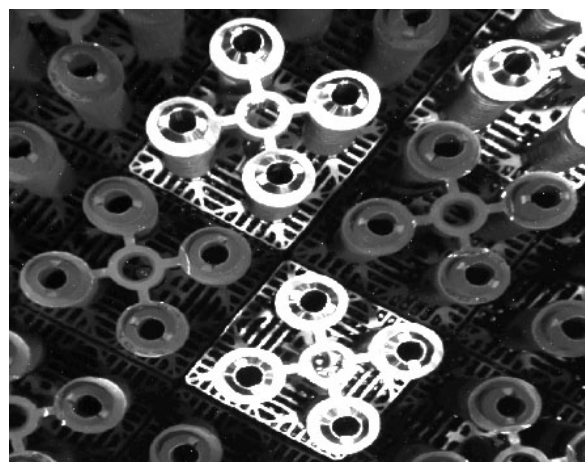


**Figure 7: Contrast between new and old fuel assemblies.**

natural features. White or retro-reflective targets are placed on points of interest on the object to be measured. A network of convergent imagery is acquired around and sometimes inside the object. Targets are readily detected in a digital image due to the marked difference in contrast with the surrounding background. The 2D image coordinates of the targets are determined via centroiding (center-of-gravity) algorithms. Coded targets and exterior orientation (EO) devices serve to automate the measurement.

A minimum number of points are measured in an image to establish the EO by resection. This is accomplished automatically by the detection in the image of either an EO device or a minimum number of coded targets, with estimated 3D coordinates. Without an EO device or coded targets, a minimum number of targets must be measured manually. Once the EO has been established, the image locations of any remaining targets with estimated 3D coordinates are predicted by projecting them into the image. This technique is known as *resection driveback.*

A calibrated artifact is typically introduced into the survey to provide scale. The coordinates of all points in all images serve as primary input to a least-squares, self-calibrating bundle adjustment. Finally, the output of the bundle consists of the adjusted 3D coordinates of all measured points of interest.

# 7 MEASUREMENT BY DETECTION OF NATURAL FEATURES

In the environment of the reactor core, operational restrictions do not permit foreign objects such as targets, EO devices, or scale artifacts. In digital imagery with sufficient contrast, the edges of the UEF plate rings can be detected to sub-pixel accuracy.

Edges in digital images are typically defined as a set of pixels that delineate an abrupt change in brightness (or intensity). Edge detection techniques are designed to find these changes. Such a change is described by a gradient that points in the direction of increasing intensity, i.e. from dark to light. Edge detection is well-documented in the fields of computer vision and photogrammetry. Many different types of edge detectors have been described in the literature. Detailed descriptions of edge detection history, theory, and techniques may be found in Faugeras (1993), Haralick and Shapiro (1992), and Mikhail et al. (2001).

Viewed under perspective, the rings of the UEF plate are imaged as ellipses. Those image points that make up a ring edge are input to a least-squares, best-fit ellipse procedure, yielding the adjusted 2D image coordinates of the ring center.

The operator initiates manual ring measurement by placing the mouse cursor at the approximate center of the ring image. All edges are detected within a window centered at the cursor position. These will likely include unwanted edges resulting from image noise, shadows, variation in object reflectivity, and the connections between rings or portions of adjoining rings that may also appear in the window (Figure 8, center). A variety of filtering techniques are applied to remove most of these unwanted edges. Remaining edge points not belonging to the ring are removed as outliers in the best-fit ellipse computation. A detected circle is seen in Figure 8 (right).

Once a minimum of four well-distributed rings have been measured across the image, the EO is determined by resection. Semi-automated measurement can be achieved by incorporating apriori information about the rings, such as radius and center-point location, into the procedure. This is similar to resection driveback described in Section 6. The 3D position of the ring center is projected into the image to predict its location. Since the radius of the ring is known, its shape and extents in the image can also be predicted. This aids in the elimination of unwanted edges. In this application, on a 2.0GHz Pentium 4 desktop computer with 512 MB of RAM, all 885 rings in one image are detected and measured in less than six seconds. As in the target approach
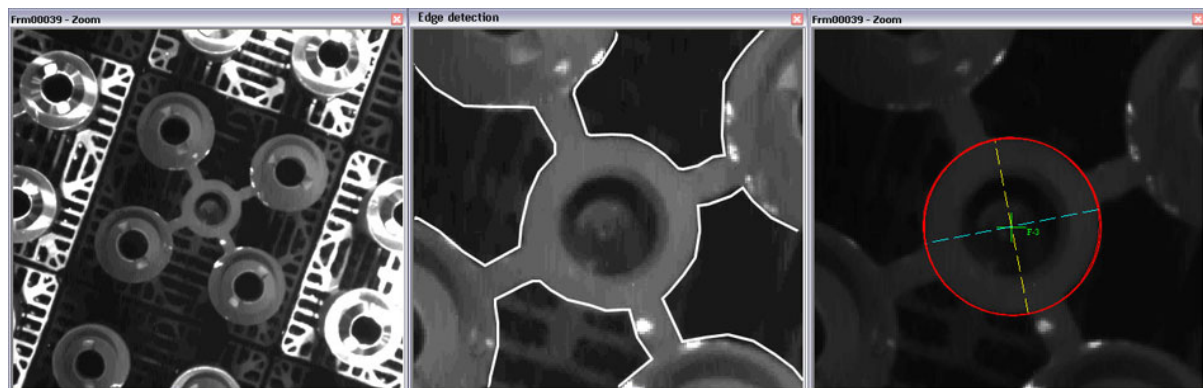


**Figure 8: Fuel assembly upper end fitting, underwater (left). Detected edges in white (center). Ellipse detected from edges ( right).**

detailed previously, the image coordinates of all ring centers in all images are input to a bundle adjustment, resulting in the adjusted 3D coordinates of the circle centers. A section of a measured image is shown in Figure 9.
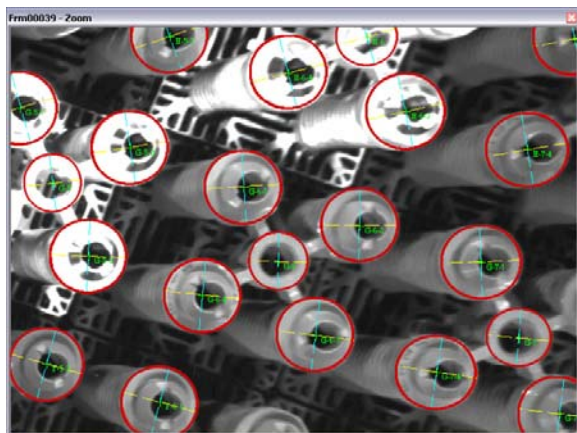
**Figure 9: Section of image showing measured ellipses.**

Each ring has an inner and an outer diameter edge. The ring center-point could be derived from either. However, as seen in Figure 9, the guide tube assembly protrudes through the four outer rings of the UEF plate. Also, the inner edge of the central ring is chamfered. Since these features may often interfere with reliable imaging of the inner diameter edge, it was decided to focus on the outer diameter edge.

## 8   MULTI-MEDIA PHOTOGRAMMETRY

Since light rays must pass through water, glass, and air prior to entering the camera lens, the issue of refraction in multi-media photogrammetry is one that must be addressed. Refractive surfaces cause light rays to deviate from the central projection resulting in image point shifts. These perturbations in image coordinates must be explicitly corrected or projectively compensated for by a self-calibrating bundle adjustment (Fraser, 1992). No attempt was made here to implement refraction correction formulae. The self-calibration approach provided results well within the desired accuracy requirements. As noted by Fraser (1992), however, self-calibration does not preclude explicit correction. Indeed, a combination of both approaches could prove to be valuable.

## 9   TEST RESULTS

In the test performed in March of 2006, a total of 52 images were collected. Of these, 46 were of sufficient quality for measurement and analysis. Some images were not utilized due to blurring caused by camera motion during acquisition. Because of operational difficulties which have since been resolved, rolls about the camera axis were minimal. For the purpose of experimentation, images were collected at more camera stations than called for in the optimal network design. In this test, all images were collected prior to measurement. Measurement and analysis were performed outside of the nuclear containment area. As the procedure becomes refined, images will be measured immediately upon

acquisition, with the final bundle adjustment performed as soon as the last image is captured. The network geometry of the survey is shown in Figure 10. One point in the middle of the field is selected to illustrate the intersection of light rays from the camera stations. Observations rejected in the bundle adjustment are indicated by red lines and accepted observations by green lines.

The nominal coordinates of all ring centers were utilized to automate the measurement as described in Section 7. In each image a minimum of four rings were measured manually and the remainder by resection driveback. Less than ten minutes were required to measure all images.

The image coordinate misclosure from the bundle adjustment was 2.35 μm. The r.m.s. of standard errors of the 885 adjusted 3D ring center coordinates were 0.123, 0.118, and 0.552 mm in X, Y, and Z, respectively.

Note that Figure 10 illustrates the narrow geometry of the bundle of rays to each point. This explains the poor accuracy in the adjusted Z coordinates. The narrow geometry is a result of the limitations on camera placement in the narrow reactor vessel. Since the primary interest is in the XY plane, Z coordinate accuracy is of little or no consequence.

The adjusted coordinates were compared to the design coordinates of the rings. Figure 11 illustrates the discrepancies between adjusted and design ring centers. As expected, the vectors from the cluster of
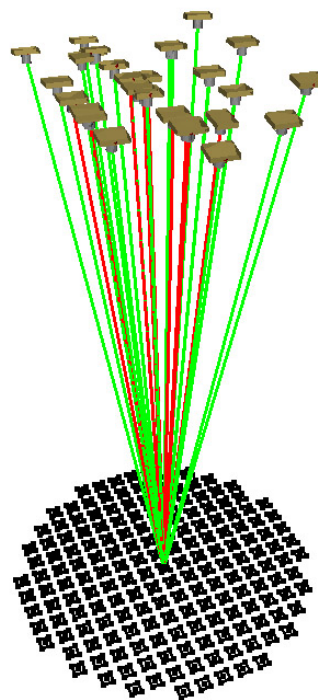


**Figure 10: Survey network geometry. Red and green lines indicate rejected and accepted observations in the bundle adjustment.**
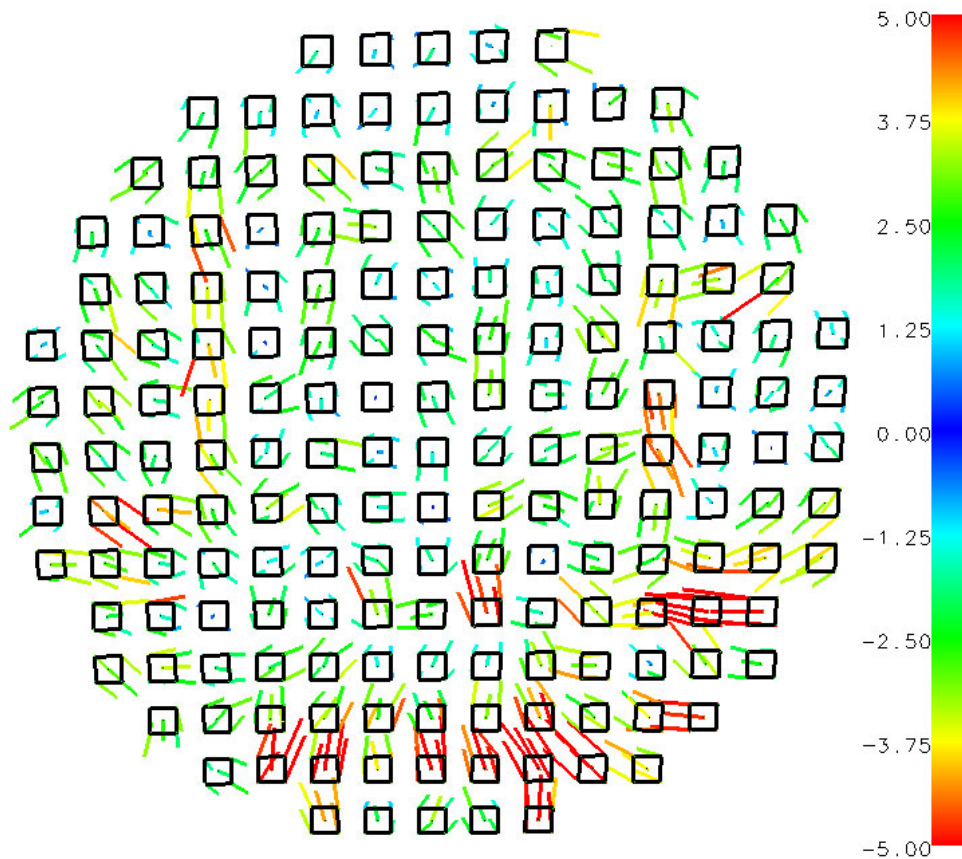
**Figure 11: Vectors representing discrepancy between adjusted and design coordinates of ring centers.**

five points on each UEF have consistent magnitude and direction.

## 10 ACCURACY ASSESSMENT

The accuracy of a photogrammetric network can be independently assessed via the measurement of some form of external standard. Typically two or more calibrated scale distances are used to scale the network and provide an independent measure of the accuracy achieved. The level of agreement between the known and measured scale distances is an indicator as to the level of accuracy achieved by the photogrammetric process. Another indicator is a comparison of the adjusted 3D coordinates to a known baseline measurement.

For this application, conventional means of accuracy assessment were not possible. No targets or scale artifacts could be placed in the reactor vessel. Design coordinates for each of the 177 UEF plates were available, but comparison to these would not necessarily provide a reliable measure of scale or accuracy.

It was decided to utilize the accurately machined UEF hold-down plates themselves as a measure of accuracy. The four computed distances between the adjusted centers of adjacent outer rings were compared to the nominal distance of 102.87 mm.

This comparison was made for each of the 177 UEF plates for a total of 708 distances. The results are shown in the table on the following page.

Rejection limits varying from 1.5 mm to 10.0 mm were applied to the difference between nominal and computed distances. Distances with differences exceeding the limit were rejected. For example, a rejection limit of 1.5 mm resulted in an r.m.s. of differences of 0.607 mm. Adjusted points associated with rejected distances were examined to establish a reason for rejection. It was found that these points belong primarily to new, shiny UEFs which were often saturated in the image. This clearly has a negative impact on circle detection and in turn, center-point determination. Future measurements would likely benefit from the acquisition of multiple exposures at each camera station.

## 11 CONCLUDING REMARKS

This paper has described the photogrammetric measurement of nuclear fuel rod assemblies by the detection of natural features. Hardware and software issues, algorithms, and practical aspects of the application have been detailed.

**Comparison of distances between nominal and adjusted UEF plate ring center points.**

| Distance Rejection Limit (mm) | Average Length (mm) | Deviation from nominal (mm) | RMS of Differences (mm) | Distances Used/Total | Percentage of Distances Used |
|---|---|---|---|---|---|
| 10.0 | 102.850 | 0.020 | 0.823 | 708/708 | 100.0 |
| 3.0 | 102.854 | 0.016 | 0.750 | 704/708 | 99.4 |
| 2.5 | 102.854 | 0.016 | 0.743 | 703/708 | 99.3 |
| 2.0 | 102.856 | 0.014 | 0.695 | 692/708 | 97.7 |
| 1.5 | 102.859 | 0.011 | 0.607 | 661/708 | 93.4 |

The results described here clearly demonstrate the suitability of computer vision techniques such as edge detection for the measurement of natural features in close-range, industrial photogrammetry. This approach shows significant potential for the measurement of not only circular objects and holes, but for slots and square shaped cutouts, and features of irregular shape. This capability is clearly valuable in many areas of manufacturing and engineering where the measurement of such features is critical, one example of which is the automotive industry.

**REFERENCES**

Faugeras, O., 1993. *Three-Dimensional Computer Vision*. Cambridge, Massachusetts: Massachusetts Institute of Technology.

Fraser, C.S., 1992. Refraction Considerations for Photogrammetric Measurements in a Thermal Vacuum Chamber. *The Photogrammetric Record*, 14(79), pp. 99-112.

Fraser, C.S., 1997. Innovations in Automation for Vision Metrology Systems. *The Photogrammetric Record*, 15(90), pp. 901-911.

Haralick, R.M. and Shapiro, L.G., 1992. *Computer and Robot Vision*. Vol. 1. Addison Wesley Publishing Company, Inc.

Mikhail, E.M., Bethel, J.S., and McGlone, J.C., 2001. *Introduction to Modern Photogrammetry*. New York: John Wiley & Sons, Inc.

Zee, S.Q., n.d. *Reactor Core and Components*, *Module 2.2.2 of Nuclear Power Reactor Technology*, Nuclear Training Center: Korean Atomic Energy Research Institute, Korea, viewed 14 May 2006, <http://www.kntc.re.kr/openlec/nuc/NPRT/>.

**ACKNOWLEDGEMENTS**